

**Electrocaloric effect in a ferroelectric  $\text{Pb}(\text{Zn}_{1/3}\text{Nb}_{2/3})\text{O}_3\text{-PbTiO}_3$  single crystal**Matjaz Valant,<sup>1</sup> Lawrence J. Dunne,<sup>2,3</sup> Anna-Karin Axelsson,<sup>3</sup> Neil McN. Alford,<sup>3</sup> George Manos,<sup>4</sup> Jani Peräntie,<sup>5</sup> Juha Hagberg,<sup>5</sup> Heli Jantunen,<sup>5</sup> and Antoni Dabkowski<sup>6</sup><sup>1</sup>*Materials Research Laboratory, University of Nova Gorica, Nova Gorica 5000, Slovenia*<sup>2</sup>*Department of Engineering Systems, London South Bank University, London SE1 0AA, United Kingdom*<sup>3</sup>*Department of Materials, Imperial College London, London SW7 2AZ, United Kingdom*<sup>4</sup>*Department of Chemical Engineering, University College London, London WC1E 7JE, United Kingdom*<sup>5</sup>*Microelectronics and Materials Physics Laboratories, University of Oulu, Oulu 90014, Finland*<sup>6</sup>*Brockhouse Institute for Materials Research, McMaster University, Hamilton, Ontario, Canada L8S 4M1*

(Received 9 April 2010; revised manuscript received 14 May 2010; published 14 June 2010)

The electrocaloric effect in a  $0.92\text{Pb}(\text{Zn}_{1/3}\text{Nb}_{2/3})\text{O}_3\text{-}0.08\text{PbTiO}_3$  single crystal was measured by a direct calorimetric technique as a function of sample temperature and electric field. The temperature of the maximum electrocaloric effect was found to coincide with the ferroelectric transition temperature. We present a theoretical description based on mean-field theory that gives a satisfactory description of the temperature and electric field dependence of the experimentally observed electrocaloric effect.

DOI: [10.1103/PhysRevB.81.214110](https://doi.org/10.1103/PhysRevB.81.214110)

PACS number(s): 77.70.+a

**I. INTRODUCTION**

The electrocaloric (EC) effect occurs when an electric field applied under adiabatic and reversible conditions changes the temperature of a polarizable material. In polar crystals, the net dipole moment and, consequently, the polarization increases with an application of an external electric field ( $E$ ). If the field is applied under adiabatic and reversible conditions, i.e., isoentropically, an increase in temperature ( $T$ ) occurs so that the total entropy ( $S$ ) remains constant such that  $S(E_1, T_1) = S(E_2, T_2)$ , where the subscripts 1 and 2 refer to initial and final states. Hence the tendency for the entropy to fall in an aligning electric field has to be compensated by a rise in temperature to keep the total entropy constant.

Early work related the electrocaloric effect to pyroelectric coefficients and the Landau theory of phase transitions.<sup>1,2</sup> More recently, there have been a range of theoretical approaches to understand the electrocaloric effect particularly in thin films.<sup>3-7</sup> If the polarization ( $P$ ) as a function of temperature is known, either experimentally or from a theoretical model the electrocaloric temperature rise can be calculated. The early work by Wiseman used the relationship,

$$(\Delta T_{\text{EC}}/\Delta E)_S = -(T/\rho C_E)(\partial P/\partial T)_E \quad (1)$$

to relate the electrocaloric temperature rise  $\Delta T_{\text{EC}}$  (assumed small otherwise an integration is required) to the change in the electric field  $\Delta E$  where  $\rho$  and  $C_E$  are the material density and heat capacity at constant electric field, respectively.<sup>8</sup> Our approach calculates the entropy directly as a function of electric field and temperature.

Other work of considerable relevance to that presented here is the transverse Ising model discussed by Cao and Li<sup>9</sup> which has been applied to  $\text{BaTiO}_3$  thin films. Four-spin exchange interactions and fluctuations are considered. Here we focus on a two-state model coupled to vibrational degrees of freedom and as appropriate for a relaxor take account of the nanodomain distribution. Prosandeev *et al.*<sup>6</sup> have used non-equilibrium molecular-dynamical techniques to study the EC

effect in bulk and low-dimensional ferroelectrics while Akcay *et al.*<sup>4,5</sup> have made theoretical investigations of the electrocaloric effect in thin films.

The first experimental measurement of the EC effect was performed on Rochelle salt and reported in 1930.<sup>10</sup> Because the temperature change was not large it was only in 1956 that the EC effect was revisited.<sup>11</sup> The investigation of EC materials gathered pace in 1960s and 1970s when a large number of dielectrics were investigated. However, the search for materials with high values of the EC effect has hardly been systematic. The EC-induced temperature change ( $\Delta T_{\text{EC}}$ ) under an external field of 25 kV/cm was generally lower than 1°. This has been the main reason that the EC effect for a long time was not considered as an alternative for a realization of a cooling process.

In recent years, research has focused on ferroelectrics and it was shown that around Curie point ( $T_C$ ) the  $\Delta T_{\text{EC}}$  can be significantly greater than other temperature regions.  $\Delta T_{\text{EC}}$  of 2.3 K was obtained for modified  $\text{PbSc}_{1/2}\text{Ta}_{1/2}\text{O}_3$  in a temperature range of  $T_C \pm 5$  K.<sup>12</sup> However, it is impossible to organize a cooling cycle in such a narrow temperature range; therefore further research has focused into systems with a diffuse ferroelectric transition such as disordered crystals, polycrystalline samples, and relaxors. In particular, relaxor ferroelectrics have recently attracted much attention. Among these, the  $\text{Pb}(\text{Mg}_{1/3}\text{Nb}_{2/3})\text{O}_3\text{-PbTiO}_3$  (PMN-PT) system is one of the most investigated.<sup>13-15</sup> A large  $\Delta T_{\text{EC}}$  of  $>1$  K for an electric field around 1.5 kV/mm has been regularly reported in a relatively wide temperature range (more than 10 K) for these ceramics and single crystals. Recently, Saranya *et al.*<sup>16</sup> reported a controversially high  $\Delta T_{\text{EC}}$  of 31 K for PMN-PT epitaxial thin films near the morphotropic phase boundary composition. They applied 18 V across a 240-nm-thick film and calculated the  $\Delta T_{\text{EC}}$  from the temperature dependence of the polarization as was done by Mischenko *et al.*<sup>17</sup> for a  $\text{PbZr}_{0.95}\text{Ti}_{0.05}\text{O}_3$  350 nm thin film (12 K at 480 kV/cm) and inferred an EC effect of 0.48 K/V. A similar study was performed on  $\text{Pb}(\text{Mg}_{1/3}\text{Nb}_{2/3})\text{O}_3\text{-PbTiO}_3$  thin films.<sup>18</sup> Unfortunately, no direct caloric measurements were made on these films.

In this paper, we report direct measurements of the electrocaloric effect in a  $\text{Pb}(\text{Zn}_{1/3}\text{Nb}_{2/3})\text{O}_3\text{-PbTiO}_3$  (PZN-PT) single crystal and give a parametrized microscopic theory of the electrocaloric effect in a model system, which reproduces the essential features of the behavior observed experimentally. To achieve this, we use a lattice model of the ferroelectric transition treated by mean-field theory and where we regard the transition as second order. Recently, we presented a microscopic theory of the EC effect in the paraelectric phase of potassium dihydrogen phosphate<sup>7</sup> but here we attempt to describe theoretically a ferroelectric system.

## II. EXPERIMENTAL PROCEDURE

Crystals of PZN-PT were grown by the solution gradient cooling technique utilizing 4" vertical tube SiC furnace. Premixed oxides were compacted in an elongated platinum crucible with conical bottom (like those used in Bridgman process) and tightly closed lid. The crucible was placed vertically in the furnace in the ceramic container partially filled with alumina powder. The ceramic tube in the furnace base delivered a controlled flow of air to the bottom tip of the crucible. After homogenization of the melt at 1160 °C, the temperature gradient in the crucible was increased by activating air cooling of the bottom tip of the crucible. This procedure during the initial stage of the process decreases the volume where the spontaneous nucleation can occur.

To further limit the of number of seeds created by the spontaneous nucleation, three oscillating-descending steps were implemented followed by slow cooling at a rate 0.5–0.75 °C/h to the termination temperature of 890 °C. From this temperature, the furnace was cooled at about 12 °C/h to room temperature.

A critical characteristic of these types of compounds is the Ti content, which was controlled by the initial composition design, based on the experimentally established effective distribution coefficient of Ti in the melt. More details about furnace design, crystal growth procedure, chemical composition control, and determination of electrical properties can be found in Ref. 19.

A single crystal with composition PZN-PT (8.4 mol %) was oriented using the Laue method (as a pseudocubic system), cut with diamond disk and polished using alumina powder (final polishing using colloidal silica) and semihard polishing cloth. The quality of the final sample was verified using polarizing light microscopy technique.

The dielectric permittivity was measured with a precision LCR meter (4284A, Hewlett-Packard/Agilent Technologies Inc.). Electrocaloric temperature measurements were performed under adiabatic conditions in a customized holder in which the sample was mounted with chromel electrode wires and polyimide adhesive tape. A chromel-alumel thermocouple was attached to one side of the sample on top of the insulating polyimide adhesive for direct temperature measurements. A dc electric field stimulus pulse lasting 3.25 s each was provided with a function generator (33120A, Agilent Technologies Inc.) via a high voltage amplifier (RT6000HVA, Radiant Technologies Inc.), and a multimeter (3457A, Agilent Technologies Inc.) was used to measure the

electrocaloric temperature response. The sample with the electrical wires was placed in a closed beaker ensuring enough long thermal time constant compared to the measurement period. The measurement was made by steplike lowering the temperature with 40 min leveling time at each temperature. Thermal loads of the electrodes, lacquer, and adhesive (~5%) were calculated to correct the direct temperature measurements. All measurements were made under computer control in an oven (UFP 400, Memmert GmbH).

## III. EXPERIMENTAL RESULTS

The quality of the grown PZN-PT single crystal, cut along (110) direction, was verified by electrical measurement. The piezoelectric coefficient  $d_{33}$  was measured to be 2300 pC/N, which is very close to reported values.<sup>20</sup> Also the measurements of dielectric constant against temperature show trends that have been described by other authors. Both phase transition temperatures correspond to published results; monoclinic to tetragonal at about 90 °C and tetragonal to cubic at around 180 °C.<sup>21</sup> The dielectric constant and characteristics of the diffuse phase transition at 180 °C also show no departure from other published results (Fig. 1).<sup>22</sup>

The measurements of the EC effect show a very small  $\Delta T_{\text{EC}}$  for monoclinic and tetragonal phases when they are much below  $T_c$ . With an increase toward  $T_c$ , the  $\Delta T_{\text{EC}}$  sharply increases and reaches the maximum exactly at the phase transition temperature. At 180 °C, the  $\Delta T_{\text{EC}}$  was measured to be 0.25 K for voltage of 1200 kV/m. The increase in the  $\Delta T_{\text{EC}}$  with voltage is not linear. For small fields, the  $\Delta T_{\text{EC}}$  increases slower than for high fields, which indicates an exponential dependence. After exceeding the  $T_c$ , the  $\Delta T_{\text{EC}}$  slowly decreases. The characteristics of the measured EC effect are very similar to characteristics of another relaxor system, i.e., the PMN-PT system.<sup>15</sup> For 1200 kV/m, the  $\Delta T_{\text{EC}}$  is around 0.1 K higher in the PMN-PT system. Because of the high  $T_c$  of the PZN-PT system, we were not able to measure the EC effect much above the transition temperature but other trends indicate that similar microscopic mechanisms are responsible for the EC effect in both systems (Fig. 2).

### Mean-field theory of the electrocaloric effect in ferroelectric PZN-PT in the vicinity of the Curie point

The end member of the PZN-PT homogeneity range is  $\text{PbTiO}_3$ , which has a perovskite structure displaying a first-order ferroelectric transition when cooling from the cubic to the tetragonal structure resulting in a sharp dielectric peak at  $T_c$ . This ferroelectric has a soft-mode-driven phase transition. By combining with a relaxor structure, such as lead zinc niobate  $\text{Pb}(\text{Zn},\text{Nb})\text{O}_3$ , broadening of the transition is observed. This is due to the structural disorder of  $\text{Zn}^{2+}$  and  $\text{Nb}^{5+}$  on the B site and local structural fluctuation between the rhombohedra and tetragonal phases within the morphotropic field, which is found to be at 8–10 %  $\text{PbTiO}_3$ . This results in formation of compositional polar nanodomains and a diffuse ferroelectric transition. By assuming a distribution of nanodomains in PZN-PT, we can rationalize the field and

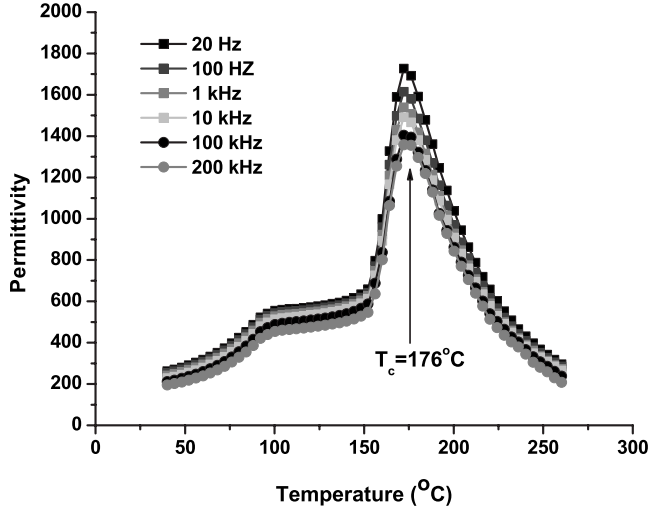


FIG. 1. Temperature dependence of permittivity for PZN-PT (110) single crystal at frequencies from 20 Hz to 200 kHz.

temperature dependence of the electrocaloric effect. The order of the transition in the PZN-PT polar nanodomains is controversial.<sup>22</sup> Here we describe it as a continuous transition in each polar nanodomain which would be difficult to distinguish from a weak first-order transition. The model is intended only to describe the EC effect around the main transition. It is not valid at much lower or higher temperatures than the Curie point as described here.

Our model is not of course an exact representation of a PZN-PT crystal but has the essential features, which allows us to describe the electrocaloric effect in these materials. A weakness which we hope to remedy in further work is that our model assumes the material does not undergo significant volume changes upon application of an electric field. Also the effective field is taken to be the macroscopic field. The model which we adopt assumes the disordered material is made up of only weakly interacting polar nanodomains

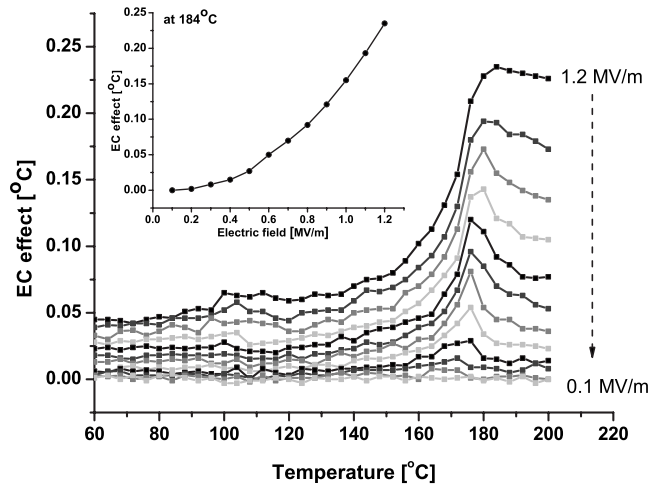


FIG. 2. Electrocaloric effect ( $\Delta T_{EC}$ ) as a function of sample temperature and for an external electric field of 100–1200 kV/m with 100 kV/m increments. The inset shows the maximum  $\Delta T_{EC}$  against the applied field.

which decouple above a weak-field limit such that they behave independently. There is considerable evidence to support the existence of polar nanodomains in PZN-PT. These polar nanodomains will be assumed to have a Gaussian distributed internal interactions as will be clarified below.

Each domain contains  $M$  mobile ions which are assumed to be able to adopt two possible up/down states in a potential provided by the effective field of neighboring atoms. Each position is associated with a dipole moment  $\mu$  (parametrized to be  $0.95 \times 10^{-30}$  C m). The average coordination is  $z$  (taken to be 4). In an electric field  $E$ , the energy of each state is  $\pm \mu E$ . Nearest-neighbor pairs of dipoles in a polar nanodomain are assumed to interact with an effective energy  $\pm J$  with the  $\pm$  signs denoting like and unlike states. The co-operative distortion mimics an attractive coupling between like dipoles.  $J$  is an average interaction energy (parametrized to be  $-113.25k$ ). The  $J$  values are assumed to be subject to a variation across the polar nanodomains which follows a Gaussian distribution. If there are  $N$  dipoles in the up orientation, the configurational energy  $E_c$  is given in a mean-field approximation by

$$E_c = \frac{zJ}{2M}(2N - M)^2 + (M - 2N)\mu E. \quad (2)$$

From Eq. (2) in zero external field, each dipole is subject to an interaction  $1/2zJ$  well below the Curie point while at this point, the interaction from neighbors goes to zero. Above the Curie point, a rapidly hopping ion has equal probability of being in either state and will appear to be on average in a centrosymmetric position.

The Canonical partition function  $Q$  is given by

$$Q(M, V, T) = q_{\text{vib}}^M \sum_N \frac{M!}{(M - N)!N!} e^{-(M - 2N)\mu E/kT} e^{-zJ(2N - M)^2/2M}. \quad (3)$$

The entropic reduction in the dipoles may be taken by any other degree of freedom. We suppose that internal partition function ( $q_{\text{vib}}$ ) of the ion vibrating in one dimension is given by

$$q_{\text{vib}} = \frac{e^{-\Theta/2T}}{1 - e^{-\Theta/T}}, \quad (4)$$

where  $\Theta$  is the Debye temperature, typically of the order of magnitude of 300 K. Defining the variable  $x = N/M$  and using the method of the maximum term where the logarithm of a sum is replaced by the logarithm of the maximum term, we obtain the Helmholtz free energy per ion ( $f_c$ ) as  $f_c = -kT \ln(Q)/M$  and is given by

$$f_c = kT[\ln(1 - x) - x \ln(1 - x) + x \ln x] - 2x\mu E + \mu E + \frac{zJ}{2}(2x - 1)^2 - kT \ln\left(\frac{e^{-\Theta/2T}}{1 - e^{-\Theta/T}}\right), \quad (5)$$

where the minimum free energy corresponds to the solution of the nonlinear equation,

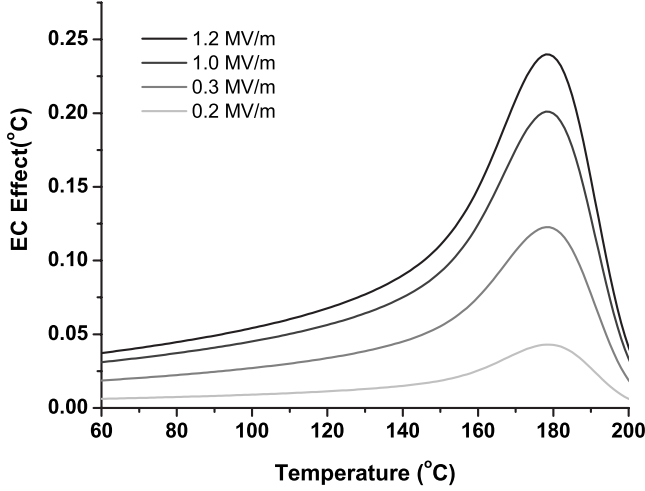


FIG. 3. Calculated EC effect as a function of sample temperature and electric field.

$$\frac{\partial f_c}{\partial x} = 0 = \frac{-2zJ(2x-1)}{kT} - \frac{2\mu E}{kT} + \ln\left(\frac{x}{1-x}\right). \quad (6)$$

The configurational entropy per ion  $S/k$  is given by

$$\frac{S}{k} = -[(1-x)\ln(1-x) + x\ln x] + \frac{\Theta/T}{e^{\Theta/T}-1} - \ln(1-e^{-\Theta/T}). \quad (7)$$

Numerical solution of Eq. (6) gives the equilibrium value of  $x$  and hence the entropy from Eq. (7). The temperature rise in an electric field can then be calculated from the condition that  $S(E_1, T_1) = S(E_2, T_2)$  using a numerical search procedure. The results are shown in Fig. 3 for four values of the electric field over a range of temperatures. The polar nanodomains are weighted according to the Gaussian distribution,

$$W(P_c) = A e^{-\beta(P_c - T_c)^2}, \quad (8)$$

where  $A$  is normalization factor,  $T_c = 453$  K,  $\beta = 0.0006$  (taken from fitting the spread of experimental data about  $T = 453$  K), and  $P_c$  is the transition temperature of a polar domain.

Figure 3 shows the calculated EC effect as a function of temperature and electric field. The model satisfactorily reproduces the essential features of the experimental observations where the electrocaloric effect peaks near the Curie point ( $T_c$ ). However, there are significant deviations at high electric fields above the Curie point.

#### IV. DISCUSSION

We have used mean-field theory in an attempt to describe the microscopic mechanisms that are responsible for the EC effect in a broad region around the Curie point of a PZN-PT crystal. It is well known that mean-field theory does not give an accurate shape of properties in the neighborhood of a transition point<sup>23</sup> and we should not expect this for our analysis. Instead, the purpose of our analysis is to describe semiquantitatively the temperature and field dependence of EC effect in this system.

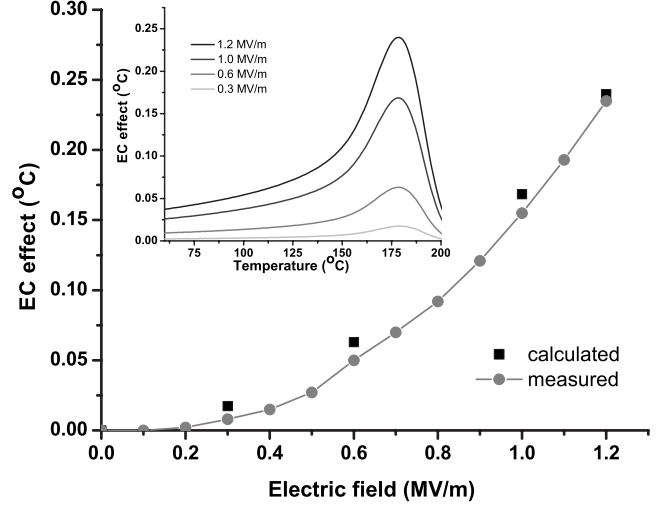


FIG. 4. Calculated and experimentally measured maximum EC effect at transition point against the electric field for the PZN-PT crystal (circles show the measured data and squares show the calculated data from the inset) with the assumption that the dipole moment is proportional to the field (see text).

From the agreement of the main characteristics of the dependencies in theory and the experiment, we conclude that the main driving force for the EC effect is the propensity of the electric field to lower the entropy of the polar system, which is compensated by a rise in vibrational entropy and temperature. Considering the crudeness of the model, it satisfactorily describes the contribution to the EC effect, which derives from the ordering of electric dipoles under the influence of an applied electric field. The calculated EC effect is the strongest at the transition temperature and it disappears gradually as the system enters the paraelectric state. In spite of the limitations of the model treated within mean-field theory,<sup>23</sup> it predicts experimental trends surprisingly well. We would like to remark that for reasons which we do not fully comprehend the agreement with experiment improved significantly by assuming a linear field dependence of the dipole moment,  $\mu = kE$  where  $k$  was fitted to be  $0.79 \times 10^{-36}$  C m<sup>2</sup> V<sup>-1</sup>. The fit of the calculated and experimentally measured maximum EC effect at transition point against the electric field is shown in Fig. 4.

#### V. CONCLUSIONS

The measured EC effect in PZN-PT single crystal is characteristic for the lead perovskite relaxor systems. The EC effect much below the transition temperature is very small and starts to increase when the transition temperature is approached. It reaches its maximum exactly at the transition temperature and, for the investigated electric fields, decreases when the system transforms to the paraelectric state. The behavior was theoretically described with mean-field theory on the basis of a model with weakly coupled nanodomains. The theory describes the experimental results in the ferroelectric phase field satisfactorily but also suggests the existence of an additional contributing mechanism at temperatures above the ferroelectric transition.



- <sup>1</sup>J. D. Childress, *J. Appl. Phys.* **33**, 1793 (1962).
- <sup>2</sup>E. Fatuzzo, H. Kiess, and R. Nitsche, *J. Appl. Phys.* **37**, 510 (1966).
- <sup>3</sup>J. H. Qiu and Q. Jiang, *J. Appl. Phys.* **105**, 034110 (2009).
- <sup>4</sup>G. Akcay, S. P. Alpay, G. A. Rossetti, Jr., and J. F. Scott, *J. Appl. Phys.* **103**, 024104 (2008).
- <sup>5</sup>G. Akcay, S. P. Alpay, J. V. Mantese, and G. A. Rossetti, *Appl. Phys. Lett.* **90**, 252909 (2007).
- <sup>6</sup>S. Prosandeev, I. Ponomareva, and L. Bellaiche, *Phys. Rev. B* **78**, 052103 (2008).
- <sup>7</sup>L. J. Dunne, M. Valant, G. Manos, A.-K. Axelsson, and N. M. Alford, *Appl. Phys. Lett.* **93**, 122906 (2008).
- <sup>8</sup>B. A. Tuttle, Ph.D. thesis, University of Illinois at Urbana-Champaign, 1981.
- <sup>9</sup>H. X. Cao and Z. Y. Li, *J. Appl. Phys.* **106**, 094104 (2009).
- <sup>10</sup>P. Kobeko and Y. Kurtschatov, *Z. Phys.* **66**, 192 (1930).
- <sup>11</sup>H. Granicher, *Helv. Phys. Acta* **29**, 210 (1956).
- <sup>12</sup>L. Shebanovs, K. Borman, W. N. Lawless, and A. Kalvane, *Ferroelectrics* **273**, 2515 (2002).
- <sup>13</sup>D. Q. Xiao, Y. C. Wang, R. L. Zhang, S. Q. Peng, J. G. Zhu, and B. Yang, *Mater. Chem. Phys.* **57**, 182 (1998).
- <sup>14</sup>L. Shaobo and L. Yanqiu, *Mater. Sci. Eng., B* **113**, 46 (2004).
- <sup>15</sup>J. Hagberg, A. Uusimäki, and H. Jantunen, *Appl. Phys. Lett.* **92**, 132909 (2008).
- <sup>16</sup>D. Saranya, A. R. Chaudhuri, J. Parui, and S. B. Krupanidhi, *Bull. Mater. Sci.* **32**, 259 (2009).
- <sup>17</sup>S. Mischenko, Q. Zhang, J. F. Scott, R. W. Whatmore, and N. D. Mathur, *Science* **311**, 1270 (2006).
- <sup>18</sup>A. S. Mischenko, Q. Zhang, R. W. Whatmore, J. F. Scott, and N. D. Mathur, *Appl. Phys. Lett.* **89**, 242912 (2006).
- <sup>19</sup>A. Dabkowski, H. A. Dabkowska, J. E. Greedan, W. Ren, and B. K. Mukherjee, *J. Cryst. Growth* **265**, 204 (2004).
- <sup>20</sup>S. E. Park and T. R. Shrout, *Mater. Res. Innovations* **1**, 20 (1997).
- <sup>21</sup>E. H. Kisi and J. S. Forrester, *J. Phys.: Condens. Matter* **20**, 165208 (2008).
- <sup>22</sup>C.-S. Tu and C.-L. Tsai, *J. Appl. Phys.* **87**, 2327 (2000).
- <sup>23</sup>K. Huang, *Statistical Mechanics*, 2nd ed. (Wiley, New York, 1963).